Vol. 23, n.°3, pp. 99-116, 2024
Revista UIS Ingenierías
https://revistas.uis.edu.co/index.php/revistauisingenierias

Technical and Environmental Evaluation of CO_2-based Booster Refrigeration Systems

Evaluación técnica y ambiental de sistemas de refrigeración tipo booster con CO_2

Daniel Vergara-Teran [1], Gustavo Aranda-Gil [2], Carlos Amaris [3]

[1] Departamento de ingeniería, Proyectos y Servicios S.A.S, Colombia. Email: vergaraterandanielenrique@gmail.com
[2] Departamento de Mantenimiento, Santa Marta Internacional Terminal Company, Colombia. Email: gustavoarandauis01@gmail.com
[3] School of Mechanical Engineering, Universidad Industrial de Santander, Colombia.
Orcid: 0000-0002-0571-282X. Email: cfamacas@uis.edu.co

Received: 15 June 2024. Accepted: 30 July 2024. Final version: 3 September 2024.

Abstract

The present study deals with the performance evaluation of four CO_2 booster refrigeration system configurations: a conventional, a parallel compressor, an ejector-based, and an NH_3/CO_2 cascade configuration, under the ambient conditions of the city of Bucaramanga, Colombia. Applying detailed energy and exergy analyses, as well as an evaluation of environmental impact through Total Equivalent Warming Impact (TEWI), it was identified that the ejector-based configuration as the most energy-efficient, exhibiting a 13.2% reduction in annual power consumption compared to the conventional system. The cascade configuration demonstrated the lowest exergy destruction above 26°C, highlighting its potential under higher ambient temperatures. Furthermore, the ejector-based configuration consistently achieved the highest 2nd law efficiency across the temperature range set. The environmental impact analysis showed the ejector-based configuration also had the lowest TEWI, with a 14.36% reduction. The results underscore the importance of selecting appropriate refrigeration configurations based on local climate conditions.

Keywords: Refrigeration; carbon dioxide; ammonia; natural refrigerants; booster refrigeration systems; energy and exergy analysis; TEWI.

Resumen

El presente estudio muestra la evaluación del rendimiento de cuatro configuraciones de sistemas de refrigeración tipo booster con CO_2: convencional, compresor en paralelo, basado en eyector y cascada con NH_3/CO_2, bajo las condiciones ambientales de la ciudad de Bucaramanga, Colombia. Aplicando un análisis detallado de energía y exergía, así como una evaluación del impacto ambiental a través del Impacto Total Equivalente de Calentamiento (TEWI), se identificó que la configuración basada en eyector es la más eficiente en términos energéticos, exhibiendo una reducción del 13.2% en el consumo anual de energía en comparación con el sistema convencional. La configuración en cascada demostró la menor destrucción de exergía por encima de los 26°C, destacando su potencial en temperaturas ambientales más altas. Además, la configuración basada en eyector logró consistentemente la mayor eficiencia de la segunda ley en todo el rango de temperatura establecido. El análisis del impacto ambiental mostró que la configuración basada en eyector también tuvo el TEWI más bajo, con una reducción del 14.36%. Los resultados subrayan la importancia de seleccionar configuraciones de refrigeración adecuadas en función de las condiciones climáticas locales.

ISSN Online: 2145 - 8456

How to cite: D. Vergara-Teran, G. Aranda-Gil, C. Amaris, "Technical and Environmental Evaluation of CO2-based Booster Refrigeration Systems," *Rev. UIS Ing.*, vol. 23, no. 3, pp. 99-116, 2024, doi: https://doi.org/10.18273/revuin.v23n3-2024009

Palabras clave: Refrigeración; dióxido de carbono; amoniaco; refrigerantes naturales; sistemas de refrigeración tipo booter; análisis energético y exergético; TEWI.

1. Introduction

The demand for more efficient and environmentally friendly refrigeration systems is becoming increasingly critical in sectors such as supermarkets, food storage, and industrial refrigeration [1]. Traditional refrigeration systems, while effective, often rely on refrigerants with high global warming potential (GWP) and consume significant amounts of energy, contributing to both environmental degradation and operational costs. As global temperatures rise and regulatory pressures increase, there is a pressing need to develop and implement advanced refrigeration technologies that not only reduce energy consumption but also minimize the environmental footprint [2].

Over the past two decades, the increasing market availability of components and accessories for natural refrigerant systems has brought renewed focus to reintroducing these refrigerants in applications where HFCs were previously dominant. These developments have called attention back to natural refrigerants such as carbon dioxide (CO_2, R744), ammonia (NH_3, R717), and hydrocarbons (R290/R600a/R1270) [3]. Moreover, the Montreal and Kyoto Protocols, along with F-Gas regulations highlighted the need to phase out and ultimately eliminate refrigerants with high GWP [4].

NH_3 is classified under the B2 safety category, indicating it is a highly toxic refrigerant with a moderate flammability risk [5]. Due to its high toxicity, NH_3 usage is restricted to certain applications where safety can be ensured. It is commonly used in industrial settings that require substantial cooling capacities. On the other hand, hydrocarbon refrigerants pose a significant flammability risk. The primary challenge in their application is the limit on the refrigerant charge per system, making hydrocarbons more suitable for small-capacity units like remote refrigerated spaces and vending machines [3]. CO_2 has become more popular compared to other natural refrigerants, especially for refrigeration in supermarket due to its negligible GWP and zero Ozone Depletion Potential (ODP) [1]. Besides its excellent environmental attributes, CO_2 boasts favourable thermophysical properties. Additionally, it is non-toxic and non-flammable across a wide range of concentrations.

A booster refrigeration system is a type of refrigeration system designed to operate efficiently under various conditions, often involving multiple stages of compression and expansion to improve performance. These systems are particularly useful in applications requiring low-temperature cooling, such as in supermarkets, food storage, and industrial refrigeration. The main advantage of a booster refrigeration system is its ability to achieve high efficiency and performance across a wide range of operating conditions, making it suitable for applications requiring both medium and low-temperature refrigeration.

When CO_2 refrigeration systems operate in warm climates as the sole refrigerant in a booster refrigeration system, the system transitions from subcritical to transcritical (or supercritical) operation. In supercritical operation, the heat rejection device functions as a gas cooler where there is not phase change, resulting in a less efficient refrigeration system. This is due to the conditions of the gas leaving the gas cooler which results in a high-quality fluid after the expansion processes. Moreover, an alternative option for supermarket refrigeration systems is the cascade system which employs two different refrigerants that operate at their own conditions to provide cooling and are connected by a heat exchanger, also called cascade heat exchanger.

Numerous studies in the open literature explore various system configurations where CO_2 is used exclusively as the refrigerant to improve system performance, even under high ambient temperature conditions [6]. Those involve configurations such as the conventional booster refrigeration system, the CO_2 cascade system, the CO_2 booster configuration featuring a gas bypass compressor (parallel compressor), and a cascade CO_2 system equipped with a gas bypass compressor [6]. Among these configurations, the CO_2 booster system with the bypass compressor was identified as the most recommended one for both moderate and warm climates. Goodarzi and Gheibi [7] investigated a two-stage transcritical CO_2 system with various design modifications. The authors concluded that the proposed refrigeration system with an internal heat exchanger showed 27% higher performance compared to conventional systems. Moreover, a sensitivity analysis on a standard CO_2 booster refrigeration configuration showed that the ambient temperature, an internal heat exchanger placed after the condenser/gas cooler, and the high-stage compressors efficiency are crucial factors for achieving optimal gas cooler pressure [8]. Other researchers have also underscored the significance of the gas cooler/condenser design, the medium temperature evaporator, and the high-stage compressor [9]–[11]. Studies have also pointed out the advantages of implementing parallel compression, dedicated sub-cooling at the gas cooler/condenser outlet [10], or multi-ejector units [12],

[13]. Mylona et al. [14] carried out a comparative study on the energy consumption and environmental impact of various refrigeration systems for frozen food supermarkets. They concluded that the CO2 booster transcritical system is the most promising alternative, given its high efficiency under London climate conditions. More recently, Gullo et al. [15] analysed the performance of a small-capacity transcritical CO_2 refrigeration unit equipped with an innovative ejector. The results showed that the ejector effectively controlled high pressure in the transcritical regime, resulting in significant COP improvements compared to existing competitors. The study highlighted the potential of the ejector to enhance energy efficiency and overall system performance in commercial refrigeration applications.

Studies on cascade refrigeration systems for food refrigeration are also available. Lee et al. [16] conducted a thermodynamic analysis of an NH_3/CO_2 cascade refrigeration configuration to identify the optimal condensing temperature at the cascade heat exchanger. The authors reported a maximum COP of 1.15 at low evaporation and condensation temperatures. Bingming et al. [17] compared the performance of an NH_3/CO_2 cascade refrigeration system with two-stage and single-stage NH_3 systems and found that the cascade configuration provided the best performance at evaporating temperatures below -40 °C among the studied conditions. Dopazo et al. [18] carried out a theoretical study on the performance of an NH_3/CO_2 cascade refrigeration configuration and reported that system COP improved as the CO_2 evaporating temperature increased and the NH_3 condensing temperature decreased. Rezayan and Behbahaninia [19] studied the thermo-economic performance of the NH_3/CO_2 cascade refrigeration cycle, reporting a 9.34% annual cost reduction compared to the base case at the studied conditions. Messineo [20] compared a basic CO_2/NH_3 cascade system with an R404A system with two-stage, concluding that both systems exhibited similar performance under the studied operating conditions. Amaris et al. [21] and Tsamos et al. [22] conducted a thermodynamic and environmental analysis of refrigeration systems, including a typical CO_2 booster configuration, a CO_2 parallel compressor booster configuration, and an NH_3/CO_2 cascade refrigeration system for retail food applications. It was demonstrated that conventional system is the recommended configuration among the studied systems at ambient temperatures up to 2 °C, while the parallel compressor configurations could provide the highest COP at ambient temperatures up to 14 °C. The cascade system showed better results at higher temperatures.

Colombia is venturing into the implementation of CO_2 refrigeration systems, with Weston SAS being a notable pioneer. By 2021, this company had completed over 15 projects in the cities such as Bogotá, Villavicencio, and Barranquilla [23]. Moreover, in 2022, the Colombian Association of Air Conditioning and Refrigeration (ACAIRE) organised the first CO_2 refrigeration training courses in Colombia [24].

In light of the aforementioned context, the current challenge presents an opportunity to propose alternative refrigeration systems to conventional Hydrofluorocarbons (HFCs), which are associated with high energy consumption and significant environmental impact. However, The performance of a specific refrigeration system varies depending on different variables such ambient temperature, system design, operating conditions, refrigerant, and control characteristics, among others [25]. Therefore, it is necessary to evaluate different configurations to provide a comprehensive understanding of how these systems perform under various climate conditions or a specific.

According to the above, there are not studies reporting the evaluation of different booster refrigeration systems at the ambient temperature variations for the city of Bucaramanga. This study aims to evaluate the performance of four CO_2 booster refrigeration system configurations (conventional, parallel compressor, ejector-based, and NH_3/CO_2 cascade booster configuration) under the ambient conditions of Bucaramanga, Colombia. By assessing the energy efficiency, exergy destruction, and 2nd law efficiency, the study seeks to identify the most energy-efficient configuration. Additionally, the study compares the annual power consumption of the different systems to determine the one offering the most significant energy savings. Furthermore, an environmental impact assessment through Total Equivalent Warming Impact (TEWI) is conducted to evaluate the potential environmental benefits of each configuration.

2. Methodology

2.1. Description of the systems

The booster refrigeration systems selected for the present study are as follows: A conventional CO_2 booster refrigeration system (see Figure 1), a parallel compression CO_2 booster refrigeration system (see Figure 2), an ejector-based CO_2 booster refrigeration system (see Figure 3), and an NH_3/CO_2 cascade booster refrigeration system (see Figure 4).

The conventional CO_2 booster refrigeration system consists of two evaporation levels, each providing the cooling effect, with two expansion devices located before the corresponding evaporator, and two compressors placed in series. The system includes one condenser/gas cooler, an expansion valve located after the condenser/gas cooler, a receiver, and a bypass valve. Each evaporator operates at different evaporation temperatures for food conservation: a maximum of 5 °C for the medium temperature (MT) evaporator and -18 °C for the low temperature (LT) evaporator.

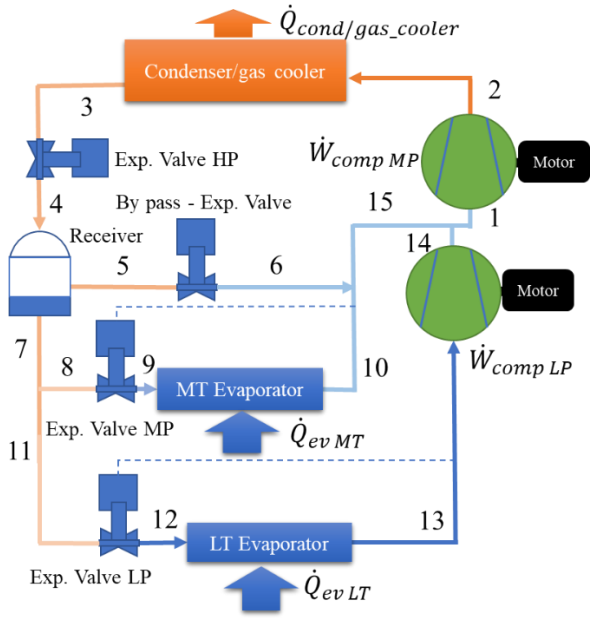

Figure 1. Diagram of the conventional CO_2 booster refrigeration system (System 1).

In this system, the superheated refrigerant vapor leaving the LT evaporator is directed to the low-pressure (LP) compressor. The refrigerant leaving the LP compressor at medium pressure is then mixed with the superheated vapor leaving the MT evaporator. The mixed flow, along with the flow from the by-pass valve, enters the medium-pressure (MP) compressor. During the compression stages, the refrigerant flows receive the required energy to reach the appropriate conditions for the heat dissipation process in the condenser/gas cooler. The condenser/gas cooler can operate as a condenser or gas cooler depending on the ambient temperature.

The refrigerant flow leaving the condenser/gas cooler expands in the high-pressure valve before entering the receiver. In the receiver, saturated liquid is sent to the MP and LP valves where it expands, while saturated vapor flows to the by-pass valve. The refrigerant flow leaving the MP and LP valves enters the corresponding evaporator as a low vapor quality mixture to initiate the evaporation process and repeat the cycle.

The parallel compression CO_2 booster refrigeration system (see Figure 2) differs from the conventional configuration by using an auxiliary compressor for the vapour flow leaving the receiver. Before entering the auxiliary compressor, the vapour flow is superheated using an Internal Heat Exchanger (IHX), which receives heat from the refrigerant flow exiting the condenser/gas cooler.

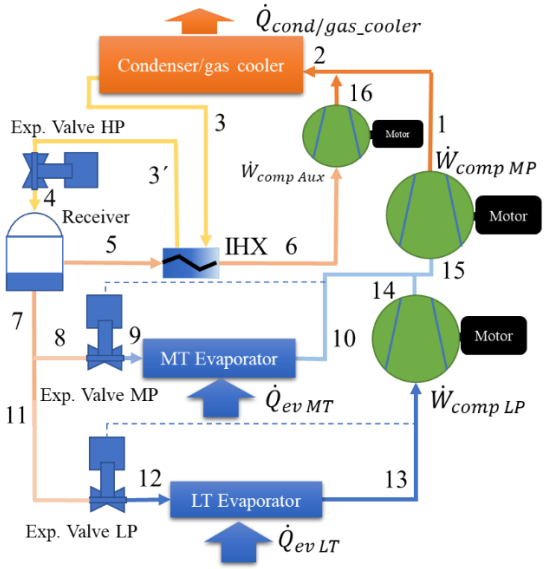

Figure 2. Diagram of the parallel compression CO_2 booster refrigeration system (System 2).

The refrigerant flow leaving the condenser/gas cooler expands in the high-pressure valve before entering the receiver. In the receiver, saturated liquid is sent to the MP and LP valves where it expands, while saturated vapor flows to the by-pass valve. The refrigerant flow leaving the MP and LP valves enters the corresponding evaporator as a low vapor quality mixture to initiate the evaporation process and repeat the cycle.

The parallel compression CO_2 booster refrigeration system (see Figure 2) differs from the conventional configuration by using an auxiliary compressor for the vapour flow leaving the receiver. Before entering the auxiliary compressor, the vapour flow is superheated using an Internal Heat Exchanger (IHX), which receives heat from the refrigerant flow exiting the condenser/gas cooler.

In the case of the ejector-based CO_2 booster refrigeration system (see Figure 3), an ejector is included to reduce the pressure ration in the MP compressor. In the ejector, a primary flow entering this component comes from the

condenser/gas cooler at the condensation pressure. A secondary flow entering the ejector comes from the mixing of the refrigerant flows leaving the LP compressor and MT evaporator. The resulting flow at the ejector outlet is a mixture, with the vapour phase sent to the MP compressor and the liquid phase sent to the MT and LT evaporators.

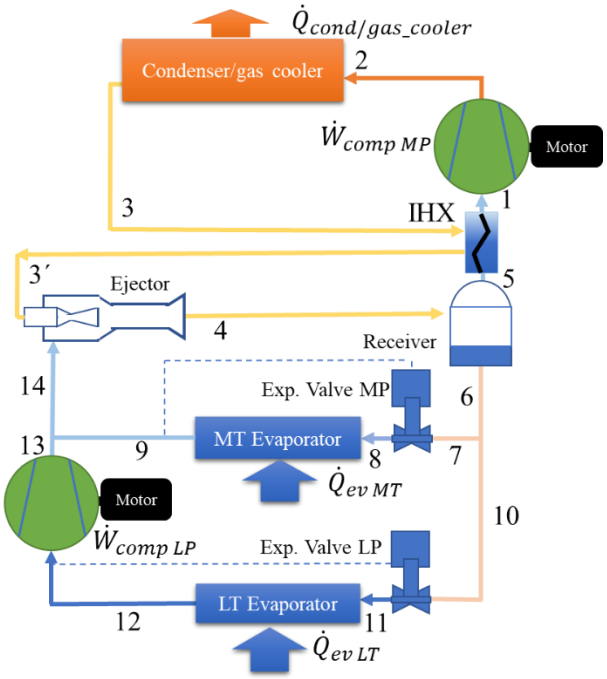

Figure 3. Diagram of the ejector-based CO_2 booster refrigeration system (System 3).

Finally, the last configuration is the NH_3/CO_2 cascade booster refrigeration system (see Figure 4), which consists of a CO_2 booster refrigeration system connected to a conventional NH_3 refrigeration system using a cascade heat exchanger. The CO_2 side refrigeration system is similar to the conventional booster system.

2.2. Model details

This section provides the procedure carried out to develop the simulation model of the evaluated systems. It includes the energy and mass balances for each component considered for the corresponding cycle, the exergy balance, operating conditions, and validation considerations.

2.2.1. Energy and mass balances

The models of the four defined systems were developed using the software Engineering Equation Solver (EES), version 11.8.

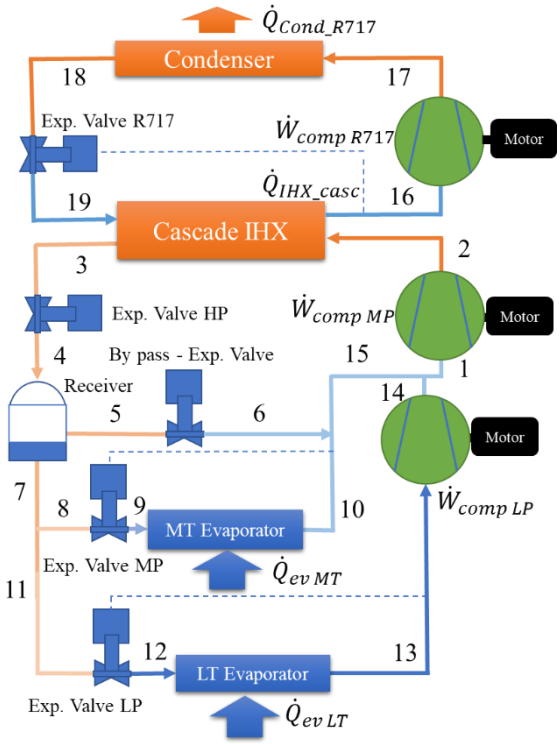

Figure 4. Diagram of the NH_3/CO_2 cascade booster refrigeration system (System 4).

The thermophysical properties of CO_2 were estimated from the database available in the EES. The energy balances for each component of the corresponding system were established as presented below:

The mass flow was estimated from the energy balances in the evaporator (Eq. 1). The heat dissipation load in the condenser/gas cooler was estimated using Eq. 2. The ideal power of the compressors was estimated using Eq. 3, while the electric power consumption was calculated considering the global efficiency in Eq. 4. Additionally, Eq. 5, 6, and 7 show the energy balances in the expansion valves, mixing points, and receivers, respectively. Eq. 8 and 9 correspond to the energy balances in the internal heat exchangers, with Eq. 8 being used to estimate the outlet temperature of the cold flow in the IHX of systems 2 and 3 (see Fig. 1b and 1c).

In the case of the ejector for the system 3, the outlet conditions were estimated using the model reported by Köhler et at. [26] and Elbel and Hrnjak [27] (Eq.11). Elbel and Hrnjak [27] expressed the efficiency of the ejector ($\eta_{Eyector}$) as the ratio between the expansion work rate recovered and the maximum possible expansion work rate. This definition coincides with that reported by Köhler et at. [26].

φ in Eq. 12 represents the ratio between the primary fluid and the secondary fluid circulating through the ejector. The performance of the systems and total energy consumption were estimated using Eq. 13 and 14, respectively.

$$\dot{m}_{in} \cdot h_{in} + \dot{Q}_{Ev} = \dot{m}_{out} \cdot h_{out} \quad (1)$$

$$\dot{m}_{in} \cdot h_{in} = \dot{m}_{out} \cdot h_{out} + \dot{Q}_{Cond.cooler} \quad (2)$$

$$\dot{m}_{in} \cdot h_{in} + \dot{W}_{Comp,s} = \dot{m}_{out} \cdot h_{out,S} \quad (3)$$

$$\dot{W}_{Comp,e} \cdot \eta_{global} = \dot{W}_{Comp,s} \quad (4)$$

$$\dot{m}_{in} \cdot h_{in} = \dot{m}_{out} \cdot h_{out} \quad (5)$$

$$\dot{m}_{1,in} \cdot h_{1,in} + \dot{m}_{2,in} \cdot h_{2,in} = \dot{m}_{out} \cdot h_{out} \quad (6)$$

$$\dot{m}_{in} \cdot h_{in} = \dot{m}_{1,out} \cdot h_{1,out} + \dot{m}_{2,out} \cdot h_{2,out} \quad (7)$$

$$\dot{m}_{c,in} \cdot h_{c,in} + \dot{Q}_{IHX} = \dot{m}_{c,out} \cdot h_{c,out} \quad (8)$$

$$\dot{m}_{h,in} \cdot h_{h,in} = \dot{Q}_{IHX} + \dot{m}_{h,out} \cdot h_{h,out} \quad (9)$$

$$\varepsilon_{IHX} = \frac{T_{c,out} - T_{c,in}}{T_{h,in} - T_{c,in}} \quad (10)$$

$$\eta_{Eyector} = \varphi \frac{h\left(P_{diff(out)}, s_{\mathrm{sec}(in)}\right) - h_{\mathrm{sec}(in)}}{h_{pri(in)} - h\left(P_{diff(out)}, s_{\mathrm{pri}(in)}\right)} \quad (11)$$

$$\varphi = \frac{\dot{m}_{sec}}{\dot{m}_{pri}} \quad (12)$$

$$COP = \frac{\dot{Q}_{MT} + \dot{Q}_{LT}}{\dot{W}_{Total}} \quad (13)$$

$$\dot{W}_{Total} = \sum \dot{W}_{comp,e} + \sum \dot{W}_{fans,lights,others} \quad (14)$$

From the above equations, $\dot{m}$ refers to the mass flow rate, h is the fluid enthalpy, $\dot{Q}_{Ev}$ is the cooling capacity, $\dot{Q}_{cond,cooler}$ refers to the heat dissipation flow, $\dot{W}_{Comp,s}$ is the ideal power consumption in the compressor, $\dot{W}_{Comp,e}$ is the electrical power consumption, and η_{global} refers to the compressor global efficiency.

The global efficiencies of the LP, MP, auxiliary, and NH_3 compressors under subcritical and supercritical conditions were correlated as a function of the pressure ratio and suction temperature as shown in Table 4. Moreover, $\dot{Q}_{HX}$ refers to the heat flow exchanged in the internal heat exchangers used in the corresponding systems. Regarding the ejector model in Eq. 11, $h\left(P_{diff(out)}, s_{\mathrm{sec}(in)}\right)$ is the ejector outlet specific enthalpy considering an isentropic state change with respect to the inlet condition of the secondary flow. $h_{\mathrm{sec}(in)}$ is the enthalpy of the secondary fluid at the ejector inlet. $h\left(P_{diff(out)}, s_{\mathrm{pri}(in)}\right)$ is the ejector outlet specific enthalpy considering an isentropic state change with respect to the inlet condition of the primary flow, and $h_{pri(in)}$ is the enthalpy of the primary fluid at the ejector inlet.

Furthermore, $\dot{Q}_{MT}$ and $\dot{Q}_{LT}$ are the medium and low temperature thermal loads in the corresponding evaporators. The total power consumption of the systems ($\dot{W}_{Total}$) includes the power consumption of the compressors plus the assumed power consumption of fans, lights, and others. In each component, the total mass flow rate fits the mass conservation, therefore, $\sum \dot{m}_{in} = \sum \dot{m}_{out}$.

2.2.2. Exergy balances

The exergy analysis by estimating the exergy destruction flow was also conducted in each component of the four configurations. The exergy destruction and efficiency according to the second law of thermodynamics were approached as follows: Eq. 15, 16, 17, and 18 represents the exergy destruction flow in the evaporators, condensers/gas coolers, expansion valves, and internal heat exchanger, respectively. Regarding Eq. 16, 17, 18, and 19, they model the exergy destruction flow in the ejector, mixing points, receivers, and compressors. The total exergy destruction in the systems for the considered components is expressed in Eq. 20. Finally, the 2nd law efficiency is given in Eq. 21.

$$\dot{X}_{Ev} = T_{amb} \cdot \left(\dot{S}_{out} - \dot{S}_{in} - \frac{\dot{Q}_{Ev}}{T_{air}}\right) \quad (15)$$

$$\dot{X}_{Cond,cooler} = T_{amb} \cdot \left(\dot{S}_{out} - \dot{S}_{in} + \frac{\dot{Q}_{Cond,cooler}}{T_{amb}}\right) \quad (16)$$

$$\dot{X}_{expd} = T_{amb} \cdot \left(\dot{S}_{out} - \dot{S}_{in}\right) \quad (17)$$

$$\dot{X}_{IHX} = T_{amb} \cdot \left(\dot{S}_{h,out} + \dot{S}_{c,out} - \dot{S}_{h,in} + \dot{S}_{c,in}\right) \quad (18)$$

$$\dot{X}_{Ej} = T_{amb} \cdot \left(\dot{S}_{out} + \dot{S}_{prim,in} - \dot{S}_{sec,in}\right) \quad (19)$$

$$\dot{X}_{Mix} = T_{amb} \cdot \left(\dot{S}_{out} + \dot{S}_{1,in} - \dot{S}_{2,in}\right) \quad (20)$$

$$\dot{X}_{Rec} = T_{amb} \cdot \left(\dot{S}_{1,out} + \dot{S}_{2,out} - \dot{S}_{in}\right) \quad (21)$$

$$\dot{X}_{comp} = \dot{W}_{comp,e} - \dot{W}_{comp,s} \quad (22)$$

$$\dot{X}_{total} = \sum \dot{X}_i \quad (23)$$

$$\eta_{ex} = 1 - \frac{\dot{X}_{total}}{\dot{W}_{Total}} \quad (24)$$

From the above equations, $\dot{S}$ refers to the total entropy flow, T_{amb} is the environmental temperature, T_{air} is the air temperature in the air side of the evaporators.

2.2.3. Environmental impact

The environmental impact of the four booster configuration was assessed by estimating the Total Equivalent Warming Impact (TEWI). The total TEWI involves the direct TEWI and indirect TEWI [28]. The direct TEWI considers the impact of refrigerant leaks, while the indirect TEWI is associated to the emissions produced due to refrigeration system energy consumption from the electrical energy generation sector for the specific country [28]. The direct TEWI is estimated by that obtained from Eq. 25 plus that obtained from Eq. 26. The indirect TEWI is approached using Eq. 27.

$$[GWP \cdot L \cdot m \cdot n] \quad (25)$$
$$[GWP \cdot m \cdot (1 - \alpha_{recovered})] \quad (26)$$
$$[n \cdot E_{anual} \cdot \beta] \quad (27)$$

Where L refers to the leakage rate in %, m is the refrigerant charge, n is the operation life of the systems in years, $\alpha_{recovered}$ is recovery factor ranging from 0 to 1, E_{anual}, is the energy consumption of the systems per year, and β refers to the indirect emission factor in kg CO_2 per kWh.

In this case, L was assumed as 15% [28], the refrigerant charge was obtained as 1.2 kg per systems cooling capacity in kW [6], n is commonly established for 10 years, $\alpha_{recovered}$ was set to 0.95 [6], [28], and β was set to 0.112378 kg CO_2 per kWh for Colombia [29].

2.2.4. Considerations and Operating conditions

The models were developed considering the next assumptions:

- Operation in steady-state.
- Potential and kinetic energies differences are negligible.
- Pressure drops considered negligible.
- Adiabatic connecting pipes.
- Processes in expansion devices are isenthalpic.
- Adiabatic ejector.

Table 1 presents the operating conditions considered for the model development.

Table 1. Base operating conditions

Parameter	Value	Unit
$\dot{Q}_{Ev,MT}$	82.8	kW
$\dot{Q}_{Ev,LT}$	23.9	kW
$T_{Ev,MT}$	-10	°C
$T_{Ev,LT}$	-32	°C
$T_{air,MT}$	5	°C
$T_{air,LT}$	-18	°C
Super heating	8	°C

The power consumption of the lights, fans, and other electrical equiptment for the gas condenser/gas cooler, MT evaporator, and LT evaporator were established as 3.7 kW, 6.9 kW, and 3.8 kW, respectively, considering the values set by Tsamos et a. [6]. The receiver pressure in the conventional, parallel, and cascade booster configurations was established as 35 Bar following the value set by Tsamos et a. [6] in their experiments.

The effectiveness of the IXH in the parallel and ejector base configuration was set to 0.14 to ensure a minimum superheating of 4 °C in the vapour entering the compressors. The condenser approach temperature difference and cascade HX temperature difference in the cascade booster configuration was set to 10 °C and 9 °C, respectively. The outlet temperature and pressure of the condenser/gas cooler was estimated considering the correlations reported by Tsamos et a. [6] for the ambient temperature range between 10 °C and 26.8 °C, and for ambient temperature values above 26.8 °C. Finally, the $\eta_{Eyector}$ for the ejector was set to 0.3 [30].

2.2.5. Models Validation procedure

Since the reliability of the models relies mainly on the power consumption estimation of the configurations for the required cooling loads, validation of the models was conducted by developing global efficiency models considering the cooling needs, power consumption, and COP reported for various compressors available in the market [31], [32]. Different compressors were selected (See Table 2) considering the required cooling capacity, evaporation temperature, and super heating shown in Table 1.

The compressor (1) for LT can provide cooling loads ranging from 6.6 kW to 40 kW for evaporation temperatures from -50 °C to -15 °C under subcritical conditions. The compressor (2) for MT can provide cooling loads ranging from 22 kW to 189 kW for evaporation temperatures from -40 °C to 0 °C under

subcritical and supercritical conditions. The compressor (3) was selected to work as auxiliary compressor considering suction temperatures between -5 and 5 °C, and cooling loads ranging from 17.9 kW and 53.8 kW. These loads were estimated from preliminary estimations of the auxiliary compressor power consumption in the system 2 and assumed COP from the manufacturer. The compressor (4) for NH_3 can provide cooling loads ranging from 44 kW to 184 kW for evaporation temperatures from -15 °C to 15 °C, considering the preliminary thermal load estimations in the cascade heat exchanger of the system 4.

Table 2. Compressors characteristics

Model	Type	Refrigerant
(1) UL-HGX24e/1105 (Subcritical)	Semi-hermetic/ Reciprocating	CO_2
(2) UL-HGX46/34541 (Supercritical)		
(3) HGX24/110-4 S T (Super critical) (Auxiliary)		
(4) F14/1166 NH_3	Open/ Reciprocating	NH_3

2.3. Bucaramanga ambient temperature details

Temperature data in the city of Bucaramanga over a 24-hour period, encompassing each month of the year. Data were collected from the meteorological station located at the Industrial University of Santander. This station provided information on dry-bulb temperature and other parameters, gathered throughout 2023. Measurements were taken every 10 minutes, spanning from 1 January to 31 December of that year. This comprehensive dataset allowed for a thorough analysis and characterisation of the city's thermal behaviour as shown in Table 3.

The data in Table 3 highlight that the most frequently occurring temperature in Bucaramanga during 2023 was approximately 23 °C, accounting for 1344.89 hours per year, which corresponds to 15.35% of the time. This is followed by a temperature of 24 °C with a frequency of 14.65%, and 25 °C with a frequency of 12.32%. These data will be used to estimate the effect of the ambient temperature on the selected systems performance and power consumption.

3. Results

This section initially provides the evaluation of the key parameter required for the validation of the models. Then, the energy and exergy analysis is presented. Finally, the environmental impact of the evaluated configuration is discussed.

Table 3. Ambient temperature data and frequency.

T_amb	# Data	# hrs/year	% time
19	31	6.13	0.07%
20	615	121.63	1.39%
21	1898	375.38	4.29%
22	4711	931.73	10.64%
23	6800	1344.89	15.35%
24	6487	1282.99	14.65%
25	5458	1079.47	12.32%
26	4359	862.12	9.84%
27	3625	716.95	8.18%
28	3363	665.13	7.59%
29	3150	623.00	7.11%
30	2234	441.84	5.04%
31	1099	217.36	2.48%
32	402	79.51	0.91%
33	55	10.88	0.12%
34	5	0.99	0.01%
Total	44292	8760.0	100%

3.1. Model validation results

The validation of the models was conducted by developing reliable correlations to estimate the power consumption of the compressors selected for the refrigeration systems (see Table 4). These correlations provide the global efficiency of the compressors as a function of the pressure ratio (PR) and the refrigerant temperature at the compressor inlet. The CO_2 LP compressor operates under subcritical conditions; however, the CO_2 MP and auxiliary compressors can operate under both subcritical and supercritical conditions. Consequently, two correlations were developed for the MP and auxiliary compressors to cover both conditions based on the data reported by the manufacturers. For the NH_3 compressor, only one correlation was required, as it operates under subcritical conditions. These global efficiency correlations were developed by initially obtaining the global efficiency using the ideal compressor power consumption and the actual power consumption available from the manufacturer for the given cooling capacity. The global efficiency of the compressors was then correlated as a function of the pressure ratio (PR) and the compressor inlet refrigerant temperature, as mentioned previously.

Figures 4a, 4b, and 4c show that the power consumption estimated (Mod) for the CO_2 LP, MP, and auxiliary

compressors using the proposed correlations presents an error deviation below 4% compared to the actual power consumption reported by the manufacturers (Man). For the NH_3 compressor, 83.3% of the data showed an error deviation below 4%, while 97.6% of the data showed an error deviation below 6.6%. These results demonstrate that the proposed correlations are suitable for estimating the compressors power consumption under the studied conditions. Regarding the ejector model validation, the model performance was previously verified by Vergara and Aranda [33].

3.2. Energy analysis

The energy analysis initially involves evaluating the power consumption, COP, and heat dissipation load as a function of ambient temperature for the four selected configurations. Subsequently, the annual total power consumption for the four configurations is presented, taking into account the variations in ambient temperature for the city of Bucaramanga.

Figure 5 shows the total power consumption of the four booster refrigeration systems as a function of ambient temperature, considering the temperature range in the city of Bucaramanga (see Table 3). As expected, the total power consumption of the four booster refrigeration systems increases as the ambient temperature rises. Furthermore, the results indicate that the conventional booster configuration has the highest total power consumption, followed by the parallel compressor booster configuration and the ejector-based booster configuration. It is also noted that the NH_3/CO_2 cascade booster configuration offers lower total power consumption than the conventional booster configuration when the ambient temperature is above 20 °C.

Table 4. Global efficiency of compressors

Compressor	Condition	Global efficiency models
LP CO_2 Comp.	Subcritical	$\eta_{global} = 0.41815 + 3.04387E\text{-}03 \cdot Tin - 6.37368E\text{-}05 \cdot Tin^2 - 1.31154E\text{-}06 \cdot Tin^3 + 0.242519 \cdot PR - 5.93520E\text{-}02 \cdot PR^2 + 4.38160E\text{-}03 \cdot PR^2$
MP CO_2 Comp.	Subcritical	$\eta_{global} = -0.239750 + 2.13770E\text{-}03 \cdot Tin - 2.40043E\text{-}05 \cdot Tin^2 - 1.76238E\text{-}06 \cdot Tin^3 - 4.38730E\text{-}08 \cdot Tin^4 + 1.10235 \cdot PR - 0.445079 \cdot PR^2 + 7.72477E\text{-}02 \cdot PR^3 - 4.88592E\text{-}03 \cdot PR^4$
	Supercritical	$\eta_{global} = 0.770911 + 2.32125E\text{-}04 \cdot Tin - 8.27663E\text{-}06 \cdot Tin^2 - 4.73126E\text{-}03 \cdot PR - 1.537929E\text{-}03 \cdot PR^2$
Aux CO_2 Comp.	Subcritical	$\eta_{global} = 3.54083E\text{-}02 - 1.26841E\text{-}03 \cdot Tin + 1.25356E\text{-}04 \cdot Tin^2 + 0.709729 \cdot PR - 0.177346 \cdot PR^2$
	Supercritical	$\eta_{global} = 0.862126 - 2.87198E\text{-}03 \cdot Tin + 1.87093E\text{-}05 \cdot Tin^2 - 3.29298E\text{-}02 \cdot PR - 6.07819E\text{-}03 \cdot PR^2$
NH_3 Comp.		$\eta_{global} = -0.469765E + 6.02941E\text{-}03 \cdot Tin + 1.43176E\text{-}04 \cdot Tin^2 - 3.69907E\text{-}06 \cdot Tin^3 + 8.60394E\text{-}01 \cdot PR - 0.217686 \cdot PR^2 + 1.81884E\text{-}02 \cdot PR^3$

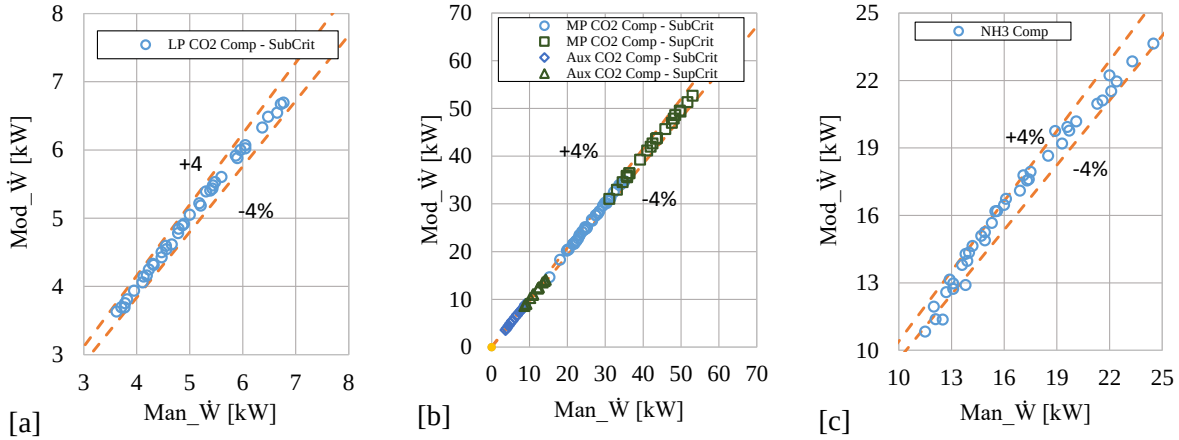

Figure 4. Modelled compressor power consumption vs power consumption reported by manufacturer for (a) LP CO_2 compressor, (b) MP and Aux CO_2 compressors, and (c) NH_3 compressor.

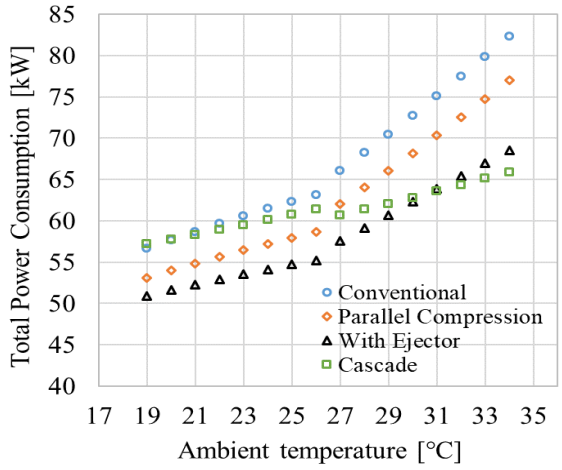

Figure 5. Booster refrigeration systems total power consumption vs ambient temperature.

Moreover, the total power consumption of the NH_3/CO_2 cascade booster configuration can be lower than that of the parallel booster configuration and the ejector-based booster configuration when the ambient temperature exceeds 26 °C and 31 °C, respectively. It is worth noting that there is a change in the trend for the conventional, parallel compressor, and ejector-based booster configurations when the ambient temperature exceeds 26 °C. This shift occurs as the booster configurations transition from operating under subcritical conditions to supercritical conditions.

Table 4 details the power consumption of the different compressors as a function of the ambient temperature given for the four booster configurations. As shown, the power consumption of the LP compressors remains constant across the defined ambient temperature range, whereas the MP compressors are notably affected by increases in ambient temperature.

Table 4 indicates that the increase in MP compressor power consumption is more significant in the conventional configuration compared to the parallel, ejector-based, and cascade configurations. Indeed, the cascade configuration offers the lowest MP compressor power consumption, followed by the parallel configuration. However, the most significant rise in power consumption for the cascade configuration is noted in the NH_3 compressor. Regarding the parallel compressor configuration, the auxiliary compressor adds additional power consumption, despite the lower MP compressor power consumption compared to the ejector-based configuration.

In any case, the auxiliary compressor in the parallel compressor configuration helps to reduce the refrigerant mass flow in the MP compressor, thereby lowering its power consumption. In the ejector-based configuration, the ejector increases the refrigerant pressure at the MP compressor inlet, resulting in a lower pressure ratio and reduced MP compressor power consumption. Since the ejector is a passive device, it does not add additional power consumption to the system. This leads to a smaller increase in MP compressor power consumption compared to the conventional MP compressor, and results in lower total power consumption compared to the conventional and parallel compressor configurations.

Figure 6 shows the COP of the four booster refrigeration systems as a function of the given ambient temperature range. Contrary to the trends for total power consumption, the COP of the four booster refrigeration systems decreases as ambient temperature rises. Furthermore, the configuration that provides the highest COP is the ejector-based booster configuration, followed by the parallel compressor booster configuration and the conventional booster configuration. The cascade booster configuration can offer a COP higher than that of the conventional booster configuration when the ambient temperature exceeds 20 °C. Additionally, the COP of the NH_3/CO_2 cascade booster configuration can be higher than that of the parallel booster configuration and the ejector-based booster configuration when the ambient temperature exceeds 26 °C and 31 °C, respectively. Since all the systems provide the same cooling capacity, the COP is directly affected by variations in total power consumption, establishing a direct correlation between the results presented in Figures 5 and 6.

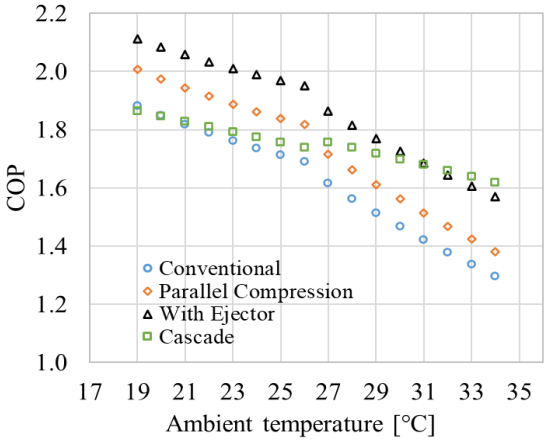

Figure 6. Booster refrigeration systems COP vs ambient temperature.

Additional simulations were conducted for lower cooling capacities as follows: 59 kW for the $\dot{Q}_{Ev,MT}$ and 17 kW for the $\dot{Q}_{Ev,LT}$, as well as 28 kW for

the $\dot{Q}_{Ev,MT}$ and 8 kW for the $\dot{Q}_{Ev,LT}$. These values were selected to simulate smaller cooling capacity CO_2 installations. In these cases, the power consumption of fans, lights, and other components was reduced proportionally with respect to the initial conditions. The simulation results for the COP of the four booster configurations indicated similar values and trends to those shown in Figure 6.

Figure 7 depicts the heat dissipation load in the condenser/gas of the four booster refrigeration systems as a function of the ambient temperature range. The figure illustrates that the highest heat dissipation load occurs in the conventional configuration, closely followed by the parallel compressor booster configuration across all the temperature range given. The heat dissipation load in the NH_3 condenser of the cascade configuration is similar to that of the conventional configuration for ambient temperatures below 27 °C. Above 27 °C, the heat dissipation load in the cascade configuration approaches that of the ejector-based configuration. The ejector-based configuration can provide the lowest heat dissipation load compared to the other configurations due to the reduction in compressor power consumption.

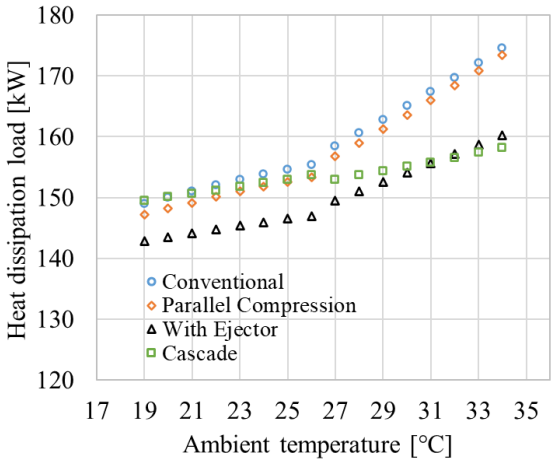

Figure 7. Booster refrigeration systems heat dissipation load vs ambient temperature.

Table 5 details the power consumption of the booster refrigeration systems based on ambient temperature frequencies for the city of Bucaramanga. For each configuration, the first column shows instantaneous total power consumption, while the second column presents the total power consumption considering annual operating hours (See Table 3) at a given ambient temperature.

The summary of the total power consumption considering annual operating hours provides the annual power consumption for each booster refrigeration system. Table 6 indicates that the power consumption of the conventional configuration, parallel compressor configuration, ejector-based configuration, and cascade configuration is estimated to be around 559,252.5 kWh/year, 522,965.4 kWh/year, 485,452.1 kWh/year, and 530,193 kWh/year, respectively, under continuous operation. Compressors in refrigeration systems do not operate continuously during the 24 hrs per day because of the on/off cycles, therefore, it is considered that the compressors could operate around 6000 per year [34]. Taking that in consideration, the power consumption of the conventional configuration, parallel compressor configuration, ejector-based configuration, and cascade configuration could be estimated to be around 383,049.66 kWh/year, 358195.48 kWh/year, 332501.44 kWh/year, and 363145.89 kWh/year, respectively, taking into account the on/off cycles. In any case, this means that the parallel compressor configuration requires an annual power consumption that is 6.5% lower than that of the conventional configuration, while the ejector-based configuration and cascade configuration have reductions of approximately 13.2% and 4.9%, respectively.

Despite the fact that the cascade booster configuration can offer a COP higher than that of the ejector-based booster configuration for ambient temperatures above 31 °C, the characteristics of the city of Bucaramanga (See Table 3) indicate that the booster configuration systems could be exposed to ambient temperatures below 31 °C around 96.5% of the time, while temperatures above 31 °C are reached only approximately 1.04% of the time.

According to the results obtained, the booster system that could provide the best performance in the city of Bucaramanga is the ejector-based booster configuration, followed by the parallel compressor booster configuration, cascade booster configuration, and lastly, the conventional booster configuration. The results presented above underline the necessity for conducting specific studies considering local ambient temperature variations and frequency to assess the performance of booster configuration systems and determine the outperforming configuration.

3.3. Exergy analysis

This subsection presents the exergy analysis for the four booster configurations. Figure 8 illustrates the exergy destruction per component for each of the four booster configurations.

Table 5. Power consumption of compressors (in kW) for each system vs ambient temperature

Ambient temperature (°C)	Conventional		Parallel Comp.			With Ejector		Cascade		
	LP	MP	LP	MP	Aux	LP	MP	LP	MP	NH3
19	4.83	37.45	4.83	26.48	7.43	4.54	31.96	4.83	18.60	19.37
20	4.83	38.47	4.83	26.90	7.88	4.54	32.66	4.83	18.60	19.92
21	4.83	39.46	4.83	27.29	8.33	4.55	33.33	4.83	18.60	20.49
22	4.83	40.42	4.83	27.66	8.79	4.55	33.97	4.83	18.60	21.07
23	4.83	41.35	4.83	28.01	9.23	4.56	34.59	4.83	18.60	21.66
24	4.83	42.24	4.83	28.34	9.67	4.56	35.17	4.83	18.60	22.26
25	4.83	43.09	4.83	28.65	10.10	4.57	35.73	4.83	18.60	22.89
26	4.83	43.90	4.83	28.93	10.51	4.57	36.25	4.83	18.60	23.53
27	4.83	46.84	4.83	31.91	10.91	4.57	38.62	4.83	17.50	23.98
28	4.83	49.02	4.83	32.87	11.95	4.58	40.16	4.83	17.50	24.65
29	4.83	51.25	4.83	33.82	13.05	4.60	41.71	4.83	17.50	25.35
30	4.83	53.52	4.83	34.75	14.21	4.61	43.26	4.83	17.50	26.07
31	4.83	55.84	4.83	35.67	15.42	4.62	44.82	4.83	17.50	26.81
32	4.83	58.20	4.83	36.58	16.71	4.63	46.38	4.83	17.50	27.58
33	4.83	60.62	4.83	37.48	18.05	4.64	47.95	4.83	17.50	28.37
34	4.83	63.08	4.83	38.37	19.46	4.65	49.52	4.83	17.50	29.19

Table 6. Annual booster refrigeration systems power consumption details

	Conventional		Parallel Compressor		With Ejector		Cascade	
T_amb [°C]	[kW]	[kWh]	[kW]	[kWh]	[kW]	[kWh]	[kW]	[kWh]
19	56.68	347.52	53.14	325.77	50.50	309.59	57.20	350.69
20	57.70	7018.28	54.01	6569.09	51.18	6225.47	57.76	7025.58
21	58.69	22031.23	54.86	20592.01	51.84	19460.61	58.33	21896.09
22	59.65	55578.86	55.68	51878.95	52.47	48890.88	58.90	54879.13
23	60.58	81470.93	56.48	75954.18	53.08	71380.20	59.49	80007.68
24	61.47	78863.99	57.24	73440.80	53.65	68828.46	60.10	77107.58
25	62.32	67274.98	57.98	62582.51	54.19	58493.46	60.72	65545.66
26	63.13	54427.11	58.67	50582.93	54.70	47154.30	61.36	52899.44
27	66.07	47365.82	62.05	44484.41	57.24	41038.76	60.71	43525.85
28	68.25	45396.38	64.05	42600.85	58.76	39084.98	61.39	40832.27
29	70.48	43909.18	66.09	41176.69	60.29	37558.92	62.08	38675.96
30	72.75	32144.53	68.19	30127.10	61.81	27311.27	62.80	27747.36
31	75.07	16317.07	70.33	15285.92	63.34	13767.89	63.55	13813.10
32	77.44	6156.62	72.52	5765.61	64.87	5157.78	64.31	5113.10
33	79.85	868.59	74.76	813.24	66.40	722.34	65.11	708.27
34	82.31	81.41	77.06	76.21	67.94	67.19	65.92	65.19
Total		559252.5 kWh/year		522965.4 kWh/year		485452.1 kWh/year		530193 kWh/year

Figure 9 depicts the efficiency of the four booster configurations according to the second law of thermodynamics.

Figure 8a shows that the most critical component in the conventional booster configuration is the MP compressor, followed by the condenser/gas cooler and the HP valve. In these components, exergy destruction increases as the ambient temperature rises, with this rise being more notable at ambient temperatures above 26°C, when the booster configuration operates under supercritical conditions. The exergy destruction in the other components increases slowly, with the effect of ambient temperature being slight.

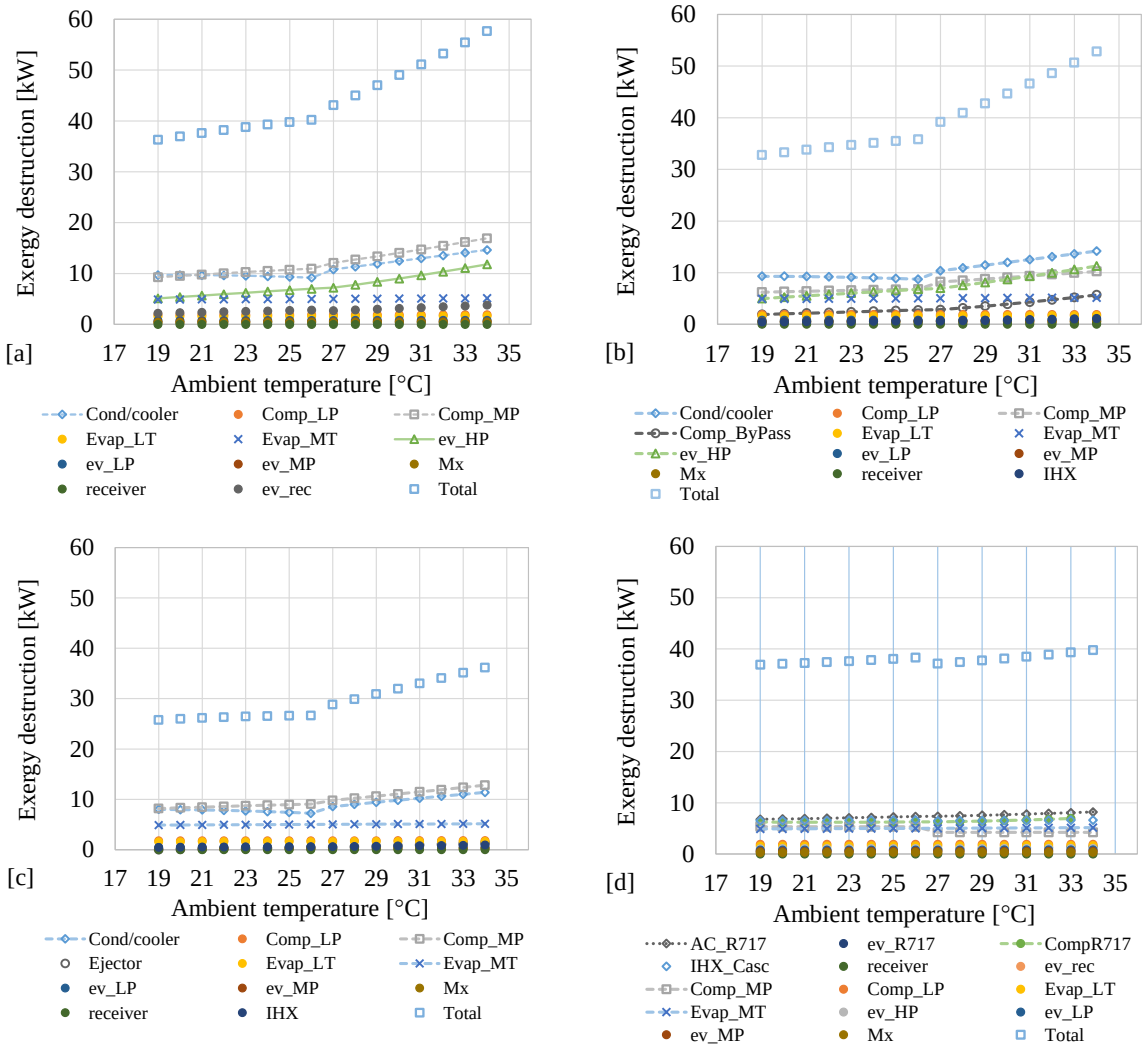

Figure 8. Booster refrigeration systems exergy destruction vs ambient temperature for [a] conventional system, [b] parallel compressor system, [c] ejector-based system, and [d] cascade system.

In the case of the parallel compressor booster configuration, Figure 8b shows that the most critical component is the condenser/gas cooler, followed by the MP compressor and the HP valve.

Comparing the total exergy destruction in the parallel compressor configuration with that in the conventional configuration, it can be noted that lower magnitudes are achieved, mainly due to a reduction in exergy destruction in the MP compressor thanks to the support of the auxiliary compressor.

Figure 8c shows that the most critical component in the ejector-based booster configuration is the MP compressor, followed by the condenser/gas cooler.

In general, the total exergy destruction in the ejector-based configuration is lower than that in the conventional, parallel compressor, and cascade configurations. This reduction is mainly due to the elimination of the HP valve and a notable decrease in exergy destruction in the MP compressor and condenser/gas cooler compared to the conventional configuration. Additionally, if the ejector is well-designed, it will not add significant exergy destruction, while helping to reduce the exergy destruction in the MP compressor.

In the case of the cascade booster configuration, figure 8d shows that the major critical component is the NH_3 condenser, followed by the NH_3 compressor. However, the magnitudes of exergy destruction are lower than those of the critical components in the other configurations.

Overall, the cascade booster configuration offers the lowest total exergy destruction compared to the conventional and parallel compressor configurations when the ambient temperature is beyond 26 °C.

Regarding the evaluation of the 2nd law efficiency, Figure 9 demonstrates that the ejector-based configuration consistently achieves the highest efficiency within the specified temperature range, primarily due to its low exergy destruction, as previously illustrated. Furthermore, all configurations exhibit a decline in efficiency as the ambient temperature increases beyond 26 °C, when the shift to supercritical conditions occurs. The parallel compressor configuration has a lower efficiency than the ejector-based configuration but higher than the conventional configuration. The cascade configuration, meanwhile, maintains relatively stable efficiency, slightly increasing until around 26 °C, after which it remains higher than both the conventional and parallel compressor configurations.

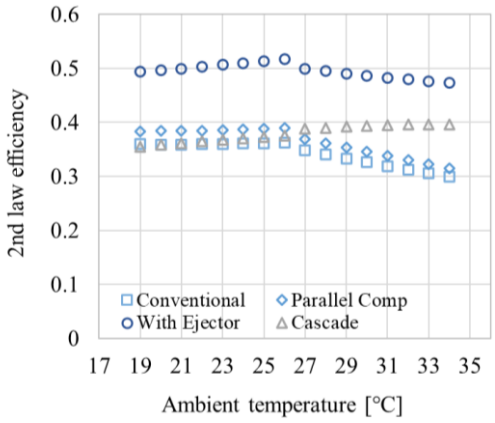

Figure 9. Booster refrigeration systems 2nd law efficiency vs ambient temperature.

3.4. Environmental impact analysis

Figure 10 illustrates the maximum Total Equivalent Warming Impact (TEWI) per ton of CO_2 equivalent for the four different booster refrigeration configurations evaluated. The TEWI values are divided into two components: Direct TEWI and Indirect TEWI.

The conventional configuration exhibits the highest total TEWI (637.2 Ton CO_2 eq.), primarily due to its high indirect TEWI, which is a result of its higher energy consumption in comparison to the other configurations.

The parallel compressor configuration shows a reduction of 7.74% in indirect TEWI compared to the conventional configuration. This reduction reflects the configuration improved energy efficiency, leading to a lower overall TEWI. The ejector-based configuration demonstrates the lowest total TEWI among all configurations with a reduction of 14.36% in indirect TEWI compared to the conventional configuration. The cascade configuration has a total TEWI around 6.46% lower than the conventional but higher than the parallel compressor and ejector-based configurations. This is due to its moderate energy efficiency improvements.

Results underscores the importance of adopting energy-efficient refrigeration systems to minimise environmental impact. The ejector-based configuration emerges as the most effective solution, offering substantial reductions in TEWI due to its lower energy consumption at the conditions of the city of Bucaramanga.

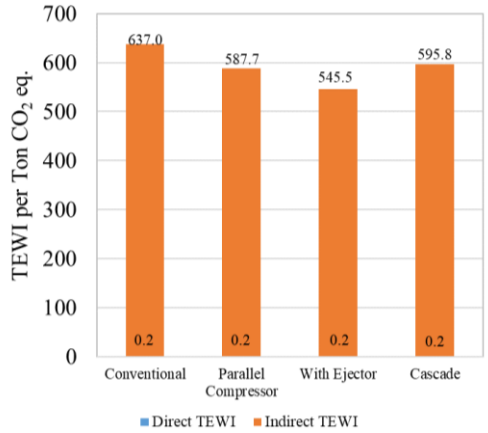

Figure 10. Environmental impact (TEWI) comparison.

4. Conclusions

This paper presented the technical and environmental evaluation of four different booster refrigeration configurations: a conventional, a parallel compressor, an ejector-based, and a cascade booster refrigeration system. The study involved an energy, exergy, 2nd law efficiency, and TEWI evaluation of the four selected configurations. The main findings of this study can be summarized as follows:

The energy analysis showed that the ejector-based booster configuration exhibits the lowest annual power consumption, achieving a reduction of 13.2% compared to the conventional configuration. The parallel compressor and cascade configurations also demonstrated significant reductions in annual power consumption by 6.5% and 4.9%, respectively.

The exergy analysis showed that the cascade booster configuration has the lowest total exergy destruction,

particularly at ambient temperatures above 26°C. The ejector-based configuration also demonstrated reduced exergy destruction, mainly due to the elimination of the HP valve and reduced destruction in the MP compressor and condenser/gas cooler. Results indicated that both the cascade and ejector-based configurations are more efficient in terms of exergy than the conventional configuration.

The 2nd law efficiency evaluation indicates that the ejector-based configuration consistently achieves the highest efficiency across the temperature range studied. All configurations show a decline in efficiency as ambient temperature rises above 26°C due to the shift to supercritical conditions. The cascade configuration maintains relatively stable efficiency, slightly increasing until around 26°C, after which it remains higher than both the conventional and parallel compressor configurations.

The TEWI analysis highlighted the environmental benefits of alternative configurations. The ejector-based configuration achieved a TEWI reduction of 14.36%, the parallel compressor configuration reduced TEWI by 7.74%, and the cascade configuration achieves a 6.46% reduction compared to the conventional configuration. The results demonstrated that the ejector-based configuration not only offers superior energy and exergy performance but also has the least environmental impact at the conditions of the city of Bucaramanga.

Future studies will be focused on evaluating additional booster refrigeration system configurations to further optimise energy and exergy performance. The study will be expanded to include the most important cities in Colombia to provide a comprehensive understanding of how different configurations perform under various climate conditions. This approach will help identify the most suitable configuration for each specific climate, ensuring optimal performance and minimal environmental impact across the country.

Funding acquisition

C. Amaris thanks the support provided by the Universidad Industrial de Santander in completing this research through the VIE No. 3771 project grant.

Autor Contributions

D. Vergara-Teran: Methodology, Investigation, Modelling, Validation, Formal Analysis, Visualization, Writing-original draft. G. Aranda-Gil: Methodology, Investigation, Modelling, Validation, Formal Analysis, Visualization, Writing-original draft. C. Amaris: Conceptualization, Methodology, Investigation, Software, Modelling, Validation, Formal Analysis, Visualization, Writing-original draft, Writing -review & editing, Supervision.

All authors have read and agreed to the published version of the manuscript.

Conflicts of Interest

The authors declare no conflict of interest.

Institutional Review Board Statement

Not applicable.

Informed Consent Statement

Not applicable.

Data availability

The data files are available on request.

References

[1] P. Gullo, K. Tsamos, A. Hafner, Y. Ge, and S. A. Tassou, "State-of-the-art technologies for transcritical R744 refrigeration systems - A theoretical assessment of energy advantages for European food retail industry," *Energy Procedia*, 2017, vol. 123, pp. 46–53, doi: https://doi.org/10.1016/j.egypro.2017.07.283

[2] J. L. Dupont, "The role of refrigeration in the global economy," *38th Informatory Note on Refrigeration Technologies*, 2019. https://iifiir.org/en/fridoc/the-role-of-refrigeration-in-the-global-economy-2019-142028

[3] C. Amaris, F. Barbosa, M. Balbis-Morejon, "Energy Performance Analysis of a Solar Refrigerator Using Ecological Refrigerants," *J. Sustain. Dev. Energy, Water Environ. Syst.*, vol. 11, no. 2, 2023, doi: https://doi.org/10.13044/j.sdewes.d11.0446

[4] E. Commission, "Regulation (EU) No 517/2014 of the European Parliament and of the Council of 16th April 2014 on Fluorinated Greenhouse Gases and Repealing Regulation (EC) No 842/2006," 2014.

[5] ISO, "ISO 5149-1:2014 Refrigerating systems and heat pumps — Safety and environmental requirements," 2014. [Online]. Available: https://www.iso.org/standard/54979.html

[6] K. M. Tsamos, Y. T. Ge, I. Santosa, S. A. Tassou, G. Bianchi, and Z. Mylona, “Energy analysis of alternative CO<inf>2</inf>refrigeration system configurations for retail food applications in moderate and warm climates,” *Energy Convers. Manag.*, vol. 150, pp. 822–829, 2017, doi: https://doi.org/10.1016/j.enconman.2017.03.020

[7] M. Goodarzi, A. Gheibi, “Performance analysis of a modified trans-critical CO2 refrigeration cycle,” *Appl. Therm. Eng.*, vol. 75, pp. 1118–1125, 2015, doi: https://doi.org/10.1016/j.applthermaleng.2014.10.075

[8] Y. T. Ge, S. A. Tassou, “Thermodynamic analysis of transcritical CO2 booster refrigeration systems in supermarket,” *Energy Convers. Manag.*, vol. 52, no. 4, pp. 1868–1875, Apr. 2011, doi: https://doi.org/10.1016/j.enconman.2010.11.015

[9] P. Gullo, B. Elmegaard, G. Cortella, “Advanced exergy analysis of a R744 booster refrigeration system with parallel compression,” *Energy*, vol. 107, pp. 562–571, Jul. 2016, doi: https://doi.org/10.1016/J.ENERGY.2016.04.043

[10] P. Gullo, B. Elmegaard, G. Cortella, “Energy and environmental performance assessment of R744 booster supermarket refrigeration systems operating in warm climates,” *Int. J. Refrig.*, vol. 64, pp. 61–79, 2016, doi: https://doi.org/10.1016/j.ijrefrig.2015.12.016

[11] K. M. Tsamos et al., “Performance investigation of the CO<inf>2</inf> gas cooler designs and its integration with the refrigeration system,” in *Energy Procedia*, vol. 123, pp. 265–272, 2017, doi: https://doi.org/10.1016/j.egypro.2017.07.237

[12] P. Gullo, K. M. Tsamos, A. Hafner, K. Banasiak, Y. T. Ge, S. A. Tassou, “Crossing CO2 equator with the aid of multi-ejector concept: A comprehensive energy and environmental comparative study,” *Energy*, vol. 164, pp. 236–263, Dec. 2018, doi: https://doi.org/10.1016/J.ENERGY.2018.08.205

[13] P. Gullo, A. Hafner, G. Cortella, “Multi-ejector R744 booster refrigerating plant and air conditioning system integration – A theoretical evaluation of energy benefits for supermarket applications,” *Int. J. Refrig.*, vol. 75, pp. 164–176, 2017, doi: https://doi.org/10.1016/J.IJREFRIG.2016.12.009

[14] Z. Mylona, M. Kolokotroni, K. M. Tsamos, S. A. Tassou, “Comparative analysis on the energy use and environmental impact of different refrigeration systems for frozen food supermarket application,” in *Energy Procedia*, vol. 123, pp. 121–130, 2017, doi: https://doi.org/10.1016/j.egypro.2017.07.234

[15] P. Gullo, M. Birkelund, E. E. Kriezi, M. R. Kærn, “Comprehensive experimental performance study on a small-capacity transcritical R744 vapour-compression refrigeration unit equipped with an innovative ejector,” *Int. J. Refrig.*, vol. 152, pp. 192–203, 2023, doi: https://doi.org/10.1016/J.IJREFRIG.2023.05.007

[16] T. S. Lee, C.-H. Liu, T. W. Chen, “Thermodynamic analysis of optimal condensing temperature of cascade-condenser in CO2/NH3 cascade refrigeration systems,” *Int. J. Refrig.*, vol. 29, no. 7, pp. 1100–1108, 2006, doi: https://doi.org/10.1016/J.IJREFRIG.2006.03.003

[17] W. Bingming, W. Huagen, L. Jianfeng, X. Ziwen, “Experimental investigation on the performance of NH3/CO2 cascade refrigeration system with twin-screw compressor,” *Int. J. Refrig.*, vol. 32, no. 6, pp. 1358–1365, 2009, doi: https://doi.org/10.1016/J.IJREFRIG.2009.03.008

[18] J. Alberto Dopazo, J. Fernández-Seara, J. Sieres, and F. J. Uhía, “Theoretical analysis of a CO2–NH3 cascade refrigeration system for cooling applications at low temperatures,” Appl. Therm. Eng., vol. 29, no. 8–9, pp. 1577–1583, Jun. 2009, doi: 10.1016/J.APPLTHERMALENG.2008.07.006.

[19] O. Rezayan, A. Behbahaninia, “Thermoeconomic optimization and exergy analysis of CO2/NH3 cascade refrigeration systems,” *Energy*, vol. 36, no. 2, pp. 888–895, Feb. 2011, doi: https://doi.org/10.1016/J.ENERGY.2010.12.022

[20] A. Messineo, “R744-R717 Cascade refrigeration system: Performance evaluation compared with a HFC two-stage system,” *in Energy Procedia*, vol. 14, pp. 56–65, 2012, doi: https://doi.org/10.1016/j.egypro.2011.12.896

[21] C. Amaris, K. M. Tsamos, and S. A. Tassou, “Analysis of an R744 typical booster configuration, an R744 parallel-compressor booster configuration and an R717/R744 cascade refrigeration system for retail food applications. Part 1: Thermodynamic analysis,” *Energy Procedia*, vol. 161, pp. 259–267, 2019, doi: https://doi.org/10.1016/j.egypro.2019.02.090

[22] K. M. Tsamos, C. Amaris, Z. Mylona, S. Tassou, "Analysis of Typical Booster Configuration, Parallel-Compressor Booster Configuration and R717/R744 Cascade Refrigeration System for Food Retail Applications. Part 2: Energy Performance in Various Climate Conditions.," *Energy Procedia*, vol. 161, pp. 268–274, 2019, doi: https://doi.org/10.1016/j.egypro.2019.02.091

[23] ACRlatinoamerica, "Weston estrena dos nuevos proyectos de CO2," 2021. https://www.acrlatinoamerica.com/2021113010149/noticias/empresas/weston-estrena-dos-nuevos-proyectos-de-co2.html

[24] ACAIRE, "Acaire inició formación en sistemas de refrigeración con CO2 transcrítico con la unidad móvil de CO2 única en sudamérica," 2022. https://acaire.org/2022/03/26/acaire-inicio-formacion-en-sistemas-de-refrigeracion-con-co2-transcritico-con-la-unidad-movil-de-co2-unica-en-sudamerica/

[25] O. A. Gelvéz-Arocha, J. E. Quiroga Méndez, D. E. Barajas-Merchán, and M. L. Gómez-Sarmiento, "Estudio experimental de las estrategias de control On-Off y control continuo en un sistema de refrigeración," *Rev. UIS Ing.*, vol. 11, no. 1, pp. 73–82, 2012.

[26] J. Köhler, C. Richter, W. Tegethoff, C. Tischendorf, "Experimental and theoretical study of a CO2 ejector refrigeration cycle," in *Vortrag, VDA Winter Meeting*, 2007.

[27] S. Elbel, P. Hrnjak, "Experimental validation of a prototype ejector designed to reduce throttling losses encountered in transcritical R744 system operation," *Int. J. Refrig.*, vol. 31, no. 3, pp. 411–422, 2008, doi: https://doi.org/10.1016/J.IJREFRIG.2007.07.013

[28] AIRAH, "Methods of calculating Total Equivalent Warming Impact (TEWI)," 2012. [Online]. Available: https://airah.org.au/Common/Uploaded files/Archive/Resources/Best_Practice_Guideline/Best_Practice_Tewi_June2012.pdf

[29] XM, "Factor de Emisión del Sistema Interconectado Nacional, para inventario de Gases de Efecto Invernadero," Noticias del Mercado, 2023. https://www.xm.com.co/noticias/5548-resultado-de-calculo-de-factor-de-emision-del-sistema-interconectado-nacional-para

[30] F. Liu, "Review on Ejector Efficiencies in Various Ejector Systems," in International Refrigeration and Air Conditioning Conference, 2014, p. 11. [Online]. Available: http://docs.lib.purdue.edu/iracc/1533

[31] Danfoss, "Compressors-for-refrigeration," Danfoss, 2024. https://www.danfoss.com/es-mx/products/dcs/compressors/compressors-for-refrigeration/#tab-product-range

[32] Bock, "Bock compressors for Stationary applications," 2024. https://vap.bock.de/stationaryapplication/Pages/Index.aspx

[33] D. Vergara-Teran, G. Aranda-Gil, "Evaluación técnica y ambiental de sistemas de refrigeración por compresión mecánica tipo booster utilizando CO2 como refrigerante natural en la ciudad de bucaramanga," trabajo de grado, Universidad Industrial de Santander, 2024.

[34] F. Fazelpour, T. Morosuk, "Exergoeconomic analysis of carbon dioxide transcritical refrigeration machines," *Int. J. Refrig.*, vol. 38, no. 1, pp. 128–139, 2014, doi: https://doi.org/10.1016/j.ijrefrig.2013.09.016